Substrate Binding and Catalysis by Ubiquitin C-Terminal Hydrolases: Identification of Two Active Site Residues†

Christopher N. Larsen, Joanne S. Price,‡ and Keith D. Wilkinson*

Department of Biochemistry, Emory University, Atlanta, Georgia 30322

Received January 16, 1996⊗

ABSTRACT: Ubiquitin C-terminal hydrolases (UCH's) are a newly-defined class of thiol proteases implicated in the proteolytic processing of polymeric ubiquitin. They are important for the generation of monomeric ubiquitin, the active component of the eukaryotic ubiquitin-dependent proteolytic system. There are at least three mammalian isozymes which are tissue specific and developmentally regulated. To study the structure and functional roles of these highly homologous enzymes, we have subcloned and overexpressed two of these isozymes, UCH-L1 and UCH-L3. Here, we report their purification, physical characteristics, and the mutagenesis of UCH-L1. Site-directed mutagenesis of UCH-L1 reveals that C90 and H161 are involved in catalytic rate enhancement. Data from circular dichroic and Raman spectroscopy, as well as secondary structure prediction algorithms, indicate that both isozymes have a significant amount of α-helix (>35%), and contain no disulfide bonds. Both enzymes are reasonably stable, undergoing a reversible thermal denaturation at 52 °C. These transitions are characterized by thermodynamic parameters typical of single domain globular proteins. Substrate binding affinity to UCH-L3 was directly measured by equilibrium gel filtration ($K_d = 0.5\ \mu$M), and the results are similar to the kinetically determined K_m for ubiquitin ethyl ester (0.6 μM). The binding is primarily electrostatic in nature and indicates the existence of a specific and extensive binding site for ubiquitin on the surface of the enzyme.

Most of the known functions of ubiquitin are mediated by the covalent conjugation of its C-terminal carboxylate to an ϵ-amino group of itself or other proteins. The post-translational formation of this isopeptide bond is implicated in cytosolic proteolysis of damaged proteins, as well as in the turnover of many short-lived regulatory proteins. Ubiquitination[1] is thought to play a role in the degradation of oncogenes and tumor suppressors, in the degradation of mitotic cyclins, in DNA repair, in receptor down-regulation, in chromosomal histone structure, in ribosome biogenesis, and in the pathogenesis of several neuronal inclusion-body diseases [reviewed by Wilkinson (1995)].

There are several polymeric ubiquitin structures which contribute to the biology of ubiquitin. Ubiquitin is post-translationally conjugated to a variety of proteins present in the cell. Proteins can be multiubiquitinated by the addition of ubiquitin to several surface lysines or polyubiquitinated by the addition of ubiquitin to one surface lysine followed by the addition of another ubiquitin to K48 of the first ubiquitin. Long polymeric chains can thus be assembled by the conjugation of ubiquitin to the distal end of this chain. These polyubiquitinated proteins are then degraded by the 26S proteasome to yield free amino acids and the polyubiquitin chain (Eytan *et al*., 1989; Hough *et al*., 1987). The ubiquitin isopeptide bond linking these subunits must be hydrolyzed by the action of specific proteases. This hydrolysis is necessary to salvage ubiquitin for further conjugation as well as to prevent the accumulation of free polyubiquitin chains which are known to bind to the 26S proteasome and inhibit proteolysis (Deveraux *et al*., 1994). We have recently shown that this reaction is catalyzed by a 93 kDa protein termed isopeptidase T (Wilkinson *et al*., 1995).

In addition to isopeptide-linked polymeric ubiquitin, the cell must also proteolytically process polymeric ubiquitin linked by peptide bonds. Ubiquitin is always translated from mRNA as a fusion protein, either with additional copies of ubiquitin itself or with one of two different zinc fingers (Ozkaynak *et al*., 1987). The proubiquitin gene product consists of multiple copies of ubiquitin, is induced by stress, and must be processed to monomeric ubiquitin by the action of a processing protease (Finley *et al*., 1987). Similarly, two ubiquitin-zinc finger fusion proteins are synthesized in rapidly growing cells. They must be accurately processed to free ubiquitin and the zinc fingers CEP52 and CEP80, which are ribosomal proteins (Finley *et al*., 1989).

The proteolytic processing of both α- and ϵ-amide linked ubiquitin occurs at the carboxyl group of glycine 76, suggesting that such processing proteases might have specificity for binding the ubiquitin monomer. Several proteases with these properties have been described, including those

† This work was supported by grants GM30308 (to K.D.W.) and 5-T32-GM08367 (to C.N.L.) from the National Institutes of Health.

* Address correspondence to this author at 4017 Rollins Research Building, Department of Biochemistry, Emory University, Atlanta, GA 30322. Tel: (404) 727-5980. FAX: (404) 727-3452. E-mail: genekdw@emory.edu.

‡ Present address: Department of Human Metabolism and Clinical Biochemistry University of Sheffield, Sheffield F10 2RX, U.K.

⊗ Abstract published in *Advance ACS Abstracts,* May 1, 1996.

[1] The nomenclature used here is as follows: Proubiquitin is the polymeric ubiquitin product of the UBI4 gene in yeast and its homologue in other eukaryotes. Ubiquitin-zinc fingers are the products of the UBI1, UBI2, and UBI3 genes in yeast and their homologues in other eukaryotes. Ubiquitination refers to the formation of isoamide bonds between the C-terminus of ubiquitin and ϵ-amino side chains of proteins. Multiubiquitination refers to the addition of a single ubiquitin to several lysines on a protein. Polyubiquitination refers to the addition of several ubiquitins to a single lysine on a protein. Polyubiquitin chains are linked by isoamide bonds between the C-terminus of ubiquitin and a lysine (usually K48) on another ubiquitin.

S0006-2960(96)00099-2 CCC: $12.00

known as ubiquitin C-terminal hydrolases (Pickart & Rose, 1985), ubiquitin specific proteases (Tobias & Varshavsky, 1991; Baker *et al*., 1992), or isopeptidases (Matsui *et al*., 1982). These proteases can be grouped into two families. The ubiquitin-specific protease family (UBP)[2] consists of several distantly-related proteases of 50−300 kDa which show several homologies around an active site thiol and a putative active site histidine. This family is also known as UCH family 2 and includes at least 11 members in yeast with other known homologues in mammals and *Drosophila* (Papa & Hochstrasser, 1993; Wilkinson *et al*., 1995). They are thought to be involved with processing various ubiquitin−protein fusions expressed in eukaryotic cells and/or the polyubiquitin degradation signal (Tobias & Varshavsky, 1991; Baker *et al*., 1992, Wilkinson *et al*., 1995). The ubiquitin carboxyl-terminal hydrolase (UCH) family is a group of small, closely-related thiol proteases consisting of three mammalian isozymes (Wilkinson *et al*., 1989) and with close homologues in *Saccharomyces cerevisae* (Liu *et al*., 1989) and *Drosophila melanogaster* (Zhang *et al*., 1993). They exhibit no apparent homology to the UBP family, and this dissimilarity implies two functionally convergent ancestral genes. The presence of multiple, tissue specific UCH isozymes (Wilkinson *et al*., 1992) suggests that the metabolism of ubiquitin may also be tissue specific. These enzymes prefer small leaving groups and/or extended peptide chains at the C-terminus of ubiquitin (unpublished observations). It is postulated that they are involved in the co-translational processing of the proubiquitin and ubiquitin-zinc finger fusion proteins which are the ubiquitin gene products. It is not clear how any of these processing proteases distinguish among the several types of polymeric ubiquitin or achieve hydrolytic specificity. Since many, if not all of them, bind ubiquitin, their hydrolytic specificities and *in vivo* rates may depend on the specific recognition of leaving group peptides, side chains, or proteins in the non-ubiquitin portion of the substrate [the P′ site according to the nomenclature of Schechter and Berger (1967)].

The UCH class of proteases is unique in several ways. Firstly, they appear to represent a new family of thiol proteases, as there is no apparent sequence homology to any other proteases. As such, the structure and function of these proteins is of general interest. Secondly, they are extremely specific, cleaving only after the C-terminal glycine of ubiquitin. Recombinant UCH's can be expressed in high amounts in *Escherichia coli*, do not form inclusion bodies, and are nontoxic to the host. This is consistent with the enzymes having a very narrow spectrum of proteolytic specificity. In contrast with members of the papain superfamily, which exhibit broad P site specificity (Fox et al., 1995), UCH's show strict and narrow P site specificities for the RGG C-terminus of Ub. Finally, these enzymes are mechanistically unique in that binding of ubiquitin results in a finite equilibrium of thiol ester between the C-terminus and the active site thiol of the protease. Thus, the enzyme−substrate complex (ubiquitin + UCH-L3) can be reduced by borohydride to give the thiohemiacetal of the protease and ubiquitin aldehyde (Pickart & Rose, 1986). The energy required to form even a small amount of intermediate thiol ester must result from extensive binding interactions between ubiquitin and the protease. For these reasons, a more detailed structural analysis of the UCH family is of interest.

We previously reported four UCH activities from bovine thymus with specificity for cleavage of the C-terminal ethyl ester of ubiquitin (Mayer & Wilkinson, 1989). Three of these enzymes are approximately 25 kDa in size, while the fourth activity is of higher molecular weight and is less well understood. These ∼25 kDa activities are named UCH-L1, UCH-L2, and UCH-L3 on the basis of their order of elution from a DE-52 anion exchange matrix, and we have found UCH-L1 to be identical to the protein PGP 9.5 (Wilkinson *et al*., 1989). This hydrolase is most highly expressed in neuronal and neurosecretory tissues. Additionally, it is selectively accumulated (along with ubiquitin conjugates) in the plaques of Alzheimer's disease as well as in lesions of other neurodegenerative diseases (Lowe *et al*., 1990). In the present work, UCH-L1 was cloned and mutagenized, and three important residues were identified, including the active site cysteine and histidine. Various spectral characterizations demonstrate that UCH contains α/β folding motifs and that the UCH mutants studied demonstrate normal parameters of thermal denaturation. Thus, these residues appear to be unimportant for protein folding or stability. As UCH-L1 is insoluble above 1.5 mg/mL, the physical characteristics of a more tractable isozyme, UCH-L3, were studied. We find that ubiquitin binding to this isozyme is stoichiometric and inhibited by salt. These data provide the first detailed analysis of the binding of ubiquitin with one of its adjunct enzymes, and so provides additional insights into the nature of the ubiquitin-UCH protein−protein binding interactions.

EXPERIMENTAL PROCEDURES

UCH Cloning and Subcloning. The cDNA encoding UCH-L3 from the plasmid pBHA (Wilkinson *et al*., 1989) was subcloned into the T7 expression vector pRSET (Invitrogen). Plasmids pBHA and pRSET were digested with *Nde*I and *Eco*RI (New England Biolabs). The 780 bp UCH-L3 insert and the 2810 bp vector were gel-purified and ligated, and the resultant plasmid was used to transform Top 10 F′ *E. coli* (Invitrogen). Colony minipreps were screened, and several which were linearized by *Nde*I to give a 3.5 kb linear fragment were selected. An insert from a positive clone was sequenced to verify the integrity of the plasmid ("pRS-UCHL3") and was used to transform the *E. coli* expression host BL21(DE3) (Novagen). On IPTG induction, cells with this plasmid overexpressed a 25 kDa protein which cross-reacted with anti-human UCH-L3 polyclonal antibodies. Cytosol from the sonicated cells showed significant enzymatic activity in cleaving ubiquitin ethyl ester (Wilkinson *et al*., 1986). Human UCH-L1 was cloned via reverse transcriptase-mediated polymerase chain reaction (RT-PCR, Perkin-Elmer Cetus) from a human fetal brain poly-A RNA library (a gift of Dr. Stephen T. Warren) using primers to the known human PGP9.5 sequence (Day *et al*., 1990). It was sequenced by the dideoxy method (Sanger *et al*., 1977), subcloned into pRSET to give pRSL1, and transformed into BL21 *E. coli* as described above. Sequencing revealed two apparent PCR errors affecting the codons for residues 73

[2] Abbreviations used: CD, circular dichroism; DTT, DL-dithiothreitol; EDTA, ethylenediaminetetraacetic acid; IPTG, isopropyl β-D-thiogalactopyranoside; MES, 2-[*N*-morpholino]ethanesulfonic acid; PAGE, polyacrylamide gel electrophoresis; PCR, polymerase chain reaction; PMSF, phenylmethylsulfonyl fluoride; SDS, sodium dodecyl sulfate; Tris, tris(hydroxymethyl)aminomethane; Ub, ubiquitin; UbOEt, ubiquitin ethyl ester (Wilkinson *et al*., 1986); UBP, ubiquitin specific proteases (Baker *et al*., 1992); UCH, ubiquitin carboxyl-terminal hydrolase (Wilkinson *et al*., 1989).

and 200. Since the change at codon 200 was silent, it was not corrected. The codon at position 73 was repaired as follows. A rat PGP9.5 (UCH-L1) fragment (Kajimoto *et al*., 1992) was amplified by PCR to generate a new silent 5′ *Bss*HII site. The resulting *Bss*HII/*Dra*III cassette codes for identical residues in the rat and the human sequences and so was inserted into pRSL1 in place of the human gene fragment. The construct was sequenced and shown to have the correct predicted amino acid sequence.

UCH Purification. We cloned, expressed, and purified recombinant UCH-L1 and UCH-L3 to study their physical and enzymatic properties. With the exceptions noted, the purification of all UCH isozymes and mutants was similar. A single colony of BL21(DE3) carrying the pRSET-UCH L3 plasmid was inoculated into 2 L of LB media (Sambrook *et al*., 1986) and grown at 37 °C to an absorbance of 0.8 at 600 nm. IPTG (Sigma) was added to 0.4 mM, and the cells were incubated for an additional 1.5 h before the bacteria were centrifuged at 4000*g* and the pellets were collected. After induction, UCH levels reached an average of 15% of the soluble *E. coli* protein. The cell paste (16 g) was resuspended in 100 mL of lysis buffer (50 mM Tris·HCl, pH 7.5, 10 mM DTT, 50 μM PMSF, 1 mM EDTA, 10 mM $MgCl_2$). Lysozyme was added to 10 000 units/mL for 30 min, and the suspension was sonicated (Heat Systems, Inc.). The debris was removed by centrifugation at 10 000*g* for 40 min. The supernatant was concentrated to 50 mL by ultrafiltration (Amicon, YM-10) and applied to a 200 mL Fast Flow Q-Sepharose column equilibrated with buffer A (50 mM Tris·HCl, pH 7.6; 0.5 mM EDTA; 5 mM DTT). The column was eluted with a 300 mL linear gradient to 0.5 M NaCl in buffer A. Fractions with ubiquitin esterase activity eluted at 265 mM NaCl and contained the 25 kDa protein as determined on SDS−PAGE. Enzymatically active fractions from ion exchange were pooled and concentrated to 30 mL and applied to a 1 L Sephadex G-100 Superfine gel filtration column (Pharmacia) in buffer A. Active fractions were pooled again and shown to be >98% pure by Coomassie-stained SDS−PAGE. These desalted enzymes have been used for kinetic studies and for the CD and UV spectroscopy, but for Raman spectra the enzymes were further purified on Mono Q FPLC anion exchange, using the same buffers and gradient as in the ion exchange step described above. The homogeneous fractions were pooled and concentrated by ultrafiltration. Purifications of UCH-L1 were similar to that for UCH-L3, except that the anion exchange salt gradients were 1−300 mM NaCl, with UCH-L1 eluting at 110 mM. Homogeneous UCH-L1 is obtained in two steps, due to slightly higher expression levels and weaker binding to Q-Sepharose. We find the specific activities of homogeneous recombinant UCH-L1 and UCH-L3 are 30 and 110 μmol/min/mg, respectively, using ubiquitin ethyl ester as the substrate. By comparison, UCH-L1 from bovine brain has a specific activity of 25 μmol/min/mg, and UCH-L3 purified from calf thymus exhibits a specific activity of approximately half the recombinant value. These enzymes are therefore fully active. Additionally, they bind one mole of substrate per mole of enzyme (see below), suggesting that they are fully functional as purified.

Mutagenesis. Mutagenesis of UCH-L1 was performed using a combination of M13-based (Kunkel, 1985), cassette subcloning, and PCR methods. In M13 mutagenesis, UCH-L1 was excised from pRSET with *Xba*I and *Hin*DIII (New England Biolabs) and inserted into M13mp18 at the same sites. Annealing, T7 polymerase extension (T7 Sequenase, USB), and ligation of primers (containing a new, silent *Hpa*I site 5′ to the mutation) with purified uracil-containing single-stranded M13 DNA generated the UCH-L1 H161D and H161Y mutants. These mutants were identified by screening plaque minipreps (Sambrook *et al*., 1986) for susceptibility to *Hpa*I digestion. The new *Hpa*I site was then used to create the mutations H161Q, H161N, and H161K: degenerate cassettes produced by PCR were inserted by their *Hpa*I and *Kpn*I sites into pRSL1 and sequenced. Lastly, C90S and D176N mutant PCR cassettes were made and inserted into the *Bss*HII and *Dra*III (C90S) or *Bss*HII and *Bsm*I sites (D176N). In all cases, the cassettes were always smaller than 400 base pairs and were sequenced after insertion into the expression vector to verify the absence of Taq polymerase-induced mutatations. All isozymes and mutants were expressed in BL21(DE3) cells, and the supernatants from lysozyme lysis were assayed. In most cases, the mutants were purified as above and their catalytic velocities and Michaelis constants were determined (Wilkinson *et al*., 1986).

UV−Vis, CD, and Raman Spectroscopy. UV−visible spectra from 190 to 800 nm were acquired on a CARY 219 dual-beam spectrophotometer. CD spectra were obtained on an Aviv Associates 62DS, using 10 or 1 mm path length quartz cuvettes (Hellma, Forest Hills, NY) at 25.0 ± 0.1 °C. Each spectrum was the average of five scan repetitions. CD spectra of the native protein were collected at 0.95 mg of protein/mL (40 μM) with 1 or 10 mm path length cells. To monitor ubiquitin binding by CD spectroscopy, ubiquitin and UCH-L3 (1 mL, 4 μM) were placed in separate compartments of a dual-compartment 9 mm cell, and the spectrum was recorded. The contents of the compartments were then mixed, and the spectrum was again recorded. The former spectrum was subtracted from the latter to give the difference binding spectrum. A similar procedure was used for determining the effects of ubiquitin binding on the UV absorbance spectra, but with UCH-L3 and ubiquitin at 20 μM.

Circular dichroic spectroscopy was used to monitor the thermal denaturation of UCH at protein concentrations of 0.1 g/L (4 μM) in 1 mm path length cells, or at 0.1 g/L in 10 mm path length cells. The latter conditions were used for the H161K and H161Y mutants, which aggregated at higher concentrations. The temperature was controlled with a Hewlett Packard 89100A temperature controller equipped with an immersible temperature probe. The temperature scan rate was varied over a 4-fold range to confirm that measurements were made at equilibrium. Scans in both directions (heating and cooling) confirmed that the transitions measured were reversible. The fraction of native protein present at each temperature was calculated assuming a two-state transition between the initial and final spectra obtained, *i.e*., at any temperature the fraction of native species = (final ellipticity − observed ellipticity)/(final ellipticity − initial ellipticity). Thermodynamic parameters were calculated from plots of ln K_{eq} vs $1/T$ or by curve fitting in Sigma Plot 4.16 for Macintosh. Equilibrium constants were used to calculate thermodynamic state functions according to $K_{eq} = \min + ((\max - \min)/(1 + 1/\exp(s - h/x)))$ where $x = T$, $s = \partial S/8.314$ J/K mol and $h = \partial H/8.314$ J/mol.

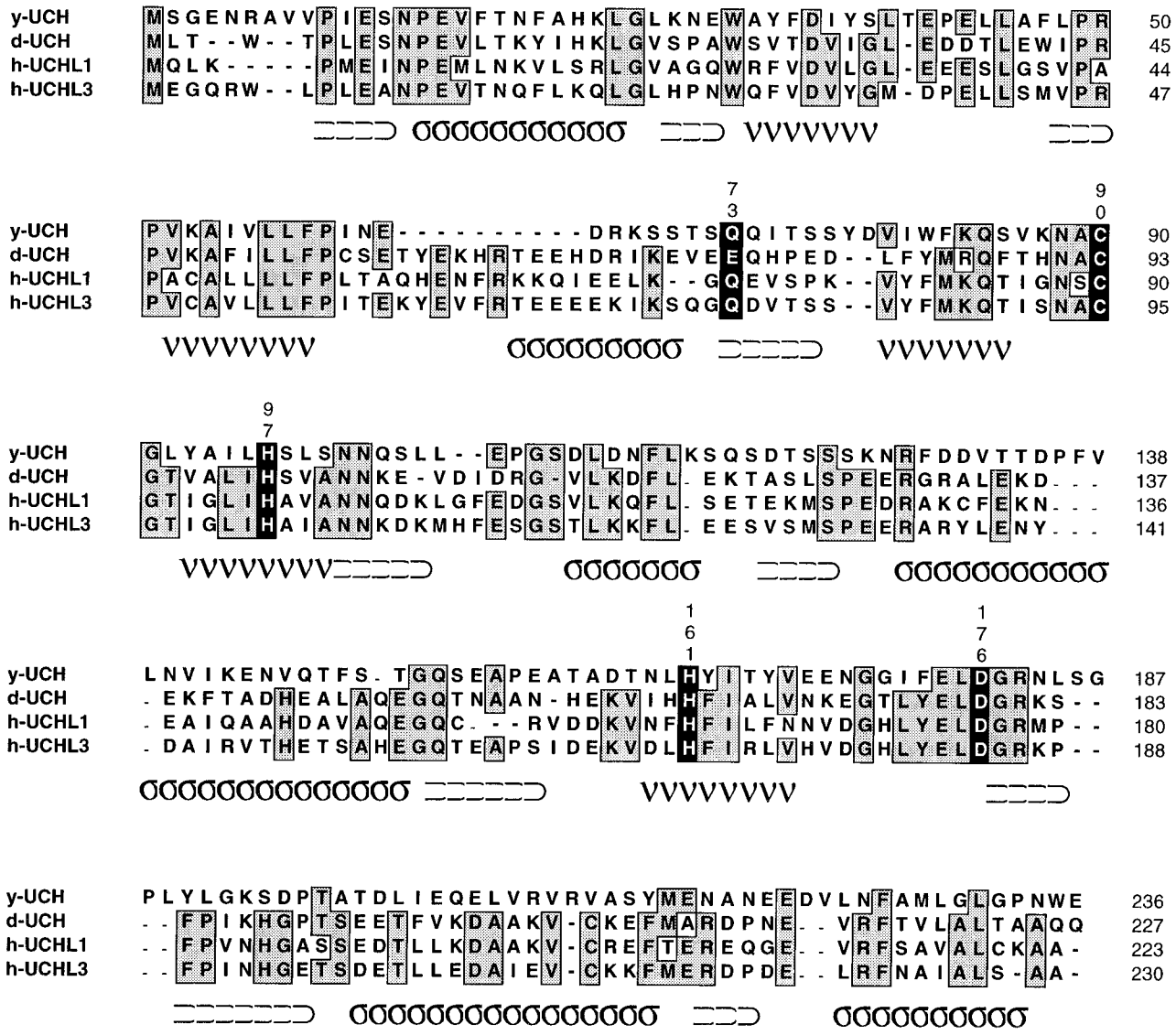

FIGURE 1: Sequence alignment of UCH isozymes. The yeast (y-UCH), *Drosophila* (d-UCH), human neuronal (h-UCH-L1), and human B-cell (h-UCH-L3) sequences are shown. Sequences were aligned using the Clustal V algorithm (Higgins & Sharp, 1989). Residues are boxed when at least three of the four sequences are identical. Underneath the alignment is shown the predicted secondary structure (helix, σ; loop, $\supset$; and β-sheet, ν) given by the neural network algorithm of the PredictProtein server (Rost & Sander, 1993).

Nonresonance Raman spectra were recorded using the 488 nm emission line of an argon laser (Spectra Physics model 165). Light scattered from the sample at 90° to the incident laser beam was dispersed by a holographic diffraction grating in a 0.6 m triple monochromator (Triplemate, Spex Industries, Metuchen, NJ) and detected by an intensified photodiode array detector (Princeton Instruments, Trenton, NJ). Power at the sample was less than 100 mW. The known Raman lines of toluene calibrated the system for each measurement, making the measured frequencies accurate to ± 1 cm^{-1}.

Equilibrium Gel Filtration. Equilibrium gel filtration measurements were performed as described (Hummel & Dreyer, 1962) with the following modifications. Tandem Superose 6 and 12 columns (0.5 × 30 cm, Pharmacia) were equilibrated with running buffer (30 mM Tris·HCl, pH 7.5; 5 mM DTT) containing 50 μg of ubiquitin/mL. After equilibration with three column volumes, the ubiquitin concentration in the effluent was identical to that in the applied buffer. Purified UCH-L3 (100 μL, 5.8 μM) was supplemented with ubiquitin to a final concentration of 50 μg/mL (5.8 μM) and applied to this column. The concentration of ligand (ubiquitin) in the effluent was determined in triplicate by HPLC using a Waters WISP 710 B autoinjector and a Gilson HPLC equipped with a Spectra Physics SP4290 integrator (Wilkinson *et al*., 1986). To determine the effect of salt on ubiquitin binding, the experiments were repeated in the presence of 0.5 M NaCl.

RESULTS AND DISCUSSION

UCH Isozyme Family. Ubiquitin C-terminal hydrolases comprise a small, newly defined, and novel family of thiol proteases. Among these, UCH-L3 is the best-characterized member. Human (Wilkinson *et al*., 1989) *Drosophila* (Zhang *et al*., 1993), and yeast (Liu *et al*., 1989) homologues have been described. These known UCH sequences are aligned in Figure 1, where only residues found in at least three sequences are highlighted. All of these enzymes have slightly acidic isoelectric points (p$I \sim 5.0$) and molecular weights between 24 and 27 kDa. The numbering system used here corresponds to the human UCH-L1 residues. A number of areas in the sequence show a high degree of

identity, most notably at positions 88−102[3] (containing a conserved cysteine), 109−118, and 161−178 (containing a conserved histidine and an ELDGR sequence). Many of the positions in the aligned sequences are identical in all four sequences (44/249) or are similar in all four (52/249). Database searches using either complete or consensus sequences have failed to identify any other significantly similar proteins.

This degree of similarity in primary sequence and physical properties is usually taken as evidence of similar secondary and tertiary structure. In support of this assumption, all four UCH sequences give essentially identical plots of Kyte−Doolittle hydropathy (data not shown). This suggests that the structural properties of these isozymes may be similar. The high homology also implies that the differential enzymatic specificity of each is a consequence of a few sequence differences at the substrate recognition site. A basal collection of UCH residues is probably necessary for proper folding and ubiquitin binding. These binding residues are expected to be on the surface of the protein and in regions that show significant sequence homology in the alignments shown in Figure 1. Additionally, catalytic residues are expected to be near the surface but are generally at the bottom of a cleft or invagination of the protein surface. To examine these relationships and make predictions about which residues to mutate, the secondary structure for this protein family has been predicted by submitting the aligned sequences shown in Figure 1 to the PredictProtein server (PredictProtein@EMBL-Heidelberg.DE). This method of prediction uses a neural net and preserves the information content of the aligned sequences, as well as that of surrounding residues rather than using only a single consensus residue at each position (Rost & Sander, 1993). These predictions (with an 82% level of confidence) are given in the last row of Figure 1 and are consistent with analyses by the Raman and circular dichroic spectroscopies discussed below.

Interestingly, the putative active site cysteine at position 90 in UCH-L1 (see below) is flanked by two putative hydrophobic β-sheet regions. These two regions of β-sheet may span from the surface of the molecule to a more protected site deeper in the molecule and position the active site thiol in the expected catalytic cleft. The cysteine is juxtaposed between the very small residues, alanine and glycine. They may allow the approach of a scissile peptide bond to form the tetrahedral intermediate. If we presume the mechanism of this protease to be papain-like, then there must also be a conserved histidine which can act as a catalytic base, polarizing the sulfhydryl and enhancing its nucleophilicity. Two positions in the UCH family have conserved histidines, these being positions 97 and 161 in UCH-L1. H97 is unlikely to be involved since it is only seven residues removed from the active site and at the opposite end of the predicted β-sheet. In contrast to papain and the serine proteases, thiol proteases of the interleukin-converting enzyme (ICE) family do not position a third residue to hydrogen bond to the catalytic histidine (Walker *et al*., 1994). Thus, it is not known if a "catalytic triad" is involved in catalysis by the UCH gene family.

UCH Expression and Purification. Recombinant proteins were expressed in *E. coli* using a modified pRSET vector (Invitrogen). The modification removed the coding region for the oligohistidine leader sequence present in the parent vector. Expression in this system is driven by a T7 RNA polymerase promoter, with induction of the polymerase by IPTG. Upon induction, the UCH isozymes and mutants were expressed at 15%−30% of the soluble protein. The enzymes were expressed, purified (see Experimental Procedures), and assayed for kinetic parameters.

[3] The amino acid numbering system refers to the UCH-L1 sequence.

Table 1: Mutagenesis and Kinetics of UCH-L1 Mutants[a]

mutant	codon change	relative rate (velocity/wt velocity)	K_m (μM)
wild type		1.00	1.20
C90S	TGT → TCT	$<1 \times 10^{-7}$	nd
H97Q	CAC → CAA	0.85	0.65
H97N	CAC → AAC	0.87	0.60
H161D	CAT → GAC	8.5×10^{-5}	1.50
H161K	CAT → AAA	$<1 \times 10^{-7}$	nd
H161N	CAT → AAC	$<1 \times 10^{-7}$	nd
H161Q	CAT → CAA	$<1 \times 10^{-7}$	nd
H161Y	CAT → TAC	$<1 \times 10^{-7}$	nd
D176N	GAT → AAT	0.025	7.40
Q73R	CAA → CGA	0.97	1.10

[a] Active mutants were purified as described for the wild type enzyme (see Experimental Procedures). Hydrolysis rates are the average of two determinations at 15 μM UbOEt, or were Michaelis constants determined according to Wilkinson *et al*. (1986). Wild type UCH-L1 velocity is 25 μmol/min/mg vs ubiquitin ethyl ester (nd: not determined).

To identify the active site residues involved in UCH catalysis, we have mutagenized the wild type UCH-L1 cDNA. The vector encoding this UCH isozyme is more tractable for mutagenesis (compared to UCH-L3) because of its greater number of useful restriction sites. Several mutants were made whose properties are summarized in Table 1. In every case, UCH-L1 mutant proteins were produced in amounts equal to the wild type enzyme, based on SDS−PAGE analysis of expression lysates. We assayed each expression lysate for activity, and active mutants were purified as described.

Physical measurements and characterization of ubiquitin binding were conducted using UCH-L3 since it was much more soluble than UCH-L1. It has also been crystallized, and structural determination by NMR and X-ray crystallography is in progress (Wilkinson *et al*., unpublished).

Identification of the Active Site Cysteine. We examined the effect of changing the putative active site thiol (C90) to a serine. This cysteine residue is conserved among all UCH's and was suspected to be involved in catalysis, though direct proof of this residues role in catalysis has not yet been shown. We generated a UCH-L1-C90S mutant (see Experimental Procedures). Assay of the bacterial lysate expressing UCH-L1-C90S showed no detectable activity. To quantitatively assess the upper limit of this activity, the C90S mutant was purified and assayed. Even at equimolar enzyme to substrate ratio (17 μM), the half-life of the substrate is over 4.5 h (not shown). Because serine is isoelectronic with cysteine, it is likely that this abrogation of activity is a direct effect and not the result of a structural change. In support of this, the C90S mutant exhibits a thermal denaturation profile with thermodynamic parameters nearly identical to the native enzyme (see below). Therefore, cysteine 90 is directly involved in catalysis, probably as the active site nucleophile.

Identification of an Active Site Histidine. We next sought to identify the active site histidine. Two positions in the alignment have a conserved histidine, corresponding to H97 and H161 in UCH-L1. To determine if these were important to catalytic function, we conservatively mutated H97 to a glutamine or asparagine. These carboxamide residues cannot provide a general base for catalytic function, but could provide hydrogen bonding similar to the N1 or N3 imidazole nitrogens and hence could provide a structural replacement. Purified UCH-L1 H97Q and H97N catalytic velocities are approximately 85% as rapid as the wild type enzyme (Table 1 and Experimental Procedures). This suggests that H97 is not involved in catalysis.

We then mutated the other fully conserved histidine at position 161. In short, all H161 mutants were either catalytically inactive or very significantly impaired. H161Q, H161N, H161Y, and H161K possess no measurable esterase activity down to the detection limit of our assay. These mutants are minimally seven orders of magnitude slower than the wild type hydrolase. Individual H161 mutations could be expected to supply an adequate structural replacement for positive electrostatic charge (lysine), hydrogen bonding by the imidazole π (asparagine) and τ (glutamine) nitrogens (Vaaler & Snell, 1989), or aromaticity and steric volume (tyrosine). Interestingly, UCH-L1 H161D shows detectable activity, about 4 orders of magnitude less than that of native enzyme. Determination of the K_m of this purified mutant showed that only the reaction rate was altered and that the K_m was unchanged (Table 1). In this context a carboxylate may function as a general base or a hydrogen bond acceptor. Either interaction would abstract proton density from the nearby cysteine thiol and enhance its nucleophilicity. Since neither H161N nor H161Q can support this level of catalysis, but could hydrogen bond, we favor a direct role for D161 as a general base. This would be the first example of a functional cys−asp dyad in a protease, though the velocity of catalysis is small. UCH-L1 H161D shows CD spectra typical of native UCH-L1 (described below), suggesting that this residue is not important for the gross enzyme structure. Our data therefore indicate that histidine 161 is intimately involved in catalysis, probably as an active site general base.

Mutation of the ELDGR Box. Because the binding of ubiquitin to UCH is primarily electrostatic (shown below), and since acid residues may be involved in catalysis, we mutated a universally conserved aspartate in the most conserved area of the UCH sequence, the ELDGR box. D176 was changed to an asparagine, resulting in a sterically unaltered charge mutant in a highly conserved region. This mutant shows a significant, measurable activity of 2.5% wild type. To determine if the drop in catalytic rate was due to an effect on binding strength, the K_m was determined (Wilkinson *et al*., 1986). Progress curve kinetics (Wilkinson *et al*., 1986; Orsi & Tipton, 1979) show this mutant to have a $K_m = 7.4\ \mu$M, approximately 6-fold weaker than that of the native enzyme. We find that the calculated specificity constant V_m/K_m is 250-fold lower than the wild type L1. Catalytic efficiency is thus lowered dramatically, but is not obliterated, and this might be expected for a residue not directly involved in catalysis. The ELDGR box may therefore be involved in the formation of a binding site or the orientation of the substrate.

Mutation of Q73. The amplification of the UCH-L1 coding sequence by RT-PCR resulted in two errors. One of these changes, a G to C transversion affecting V200, was silent and was not repaired. Another G to A transition generated the mutant Q73R. We repaired the R73 mutation by replacing the defective region with a fragment from the rat UCH-L1 cDNA. Both rat and human proteins have identical sequences in this region (Kajimoto *et al*., 1992; Day *et al*., 1990), and the swap thus repaired the original PCR mutation (Experimental Procedures). Residue 73 is 17 residues N-terminal to the active site cysteine. It is predicted to be at the surface of the enzyme, possibly as part of a turn at the opposite end of the β-sheet anchoring the active site cysteine. Since all known UCH sequences have a Q in this region (equivalent to either position 73 or 74 in UCH-L1), it was of interest to examine the catalytic activity of this mutant. Table 1 shows that mutation of this position to the positively charged R residue had no effect on the activity of the enzyme or its affinity for substrate.

Structural Effects of These Mutations. To ensure that the lack of activity in these mutants was not due to gross structural misfolding of the enzymes, we analyzed selected mutants by circular dichroism. UCH-L1 mutants Q73R, H161D, D176N, and C90S all show CD spectra typical of UCH-L1 (described below), suggesting that these residues are not important for the gross enzyme structure. All of these mutants were expressed at levels similar to the wild type, again suggesting that folding and solubility were not problems with these specific mutations.

Binding of Ubiquitin to UCH-L3. To characterize the ubiquitin binding site and to identify any structural changes and/or perturbation of the environment of amino acid side chains associated with the binding of ubiquitin to UCH, we have studied the spectral properties of the more soluble isozyme, UCH-L3, upon binding of ubiquitin. Circular dichroism has previously been used to monitor protein−protein interactions accompanied by conformational changes, as well as to examine the environment of aromatic residues (Beltramini *et al*., 1992; Blazy *et al*., 1992; Grobler *et al*., 1994; Vuillemier *et al*., 1993). We purified UCH-L3 (Experimental Procedures) and used it to study substrate binding by various approaches. We were unable to detect any changes of ellipticity in CD difference spectra upon binding of ubiquitin and UCH-L3. This suggests that the structure of the two proteins are not altered by binding, such that no gross "induced fit" conformational changes are detectable.

To examine if aromatic residues were perturbed by substrate binding, the UV spectra of Ub and UCH-L3 were recorded in dual-compartment cells. After the compartment contents were mixed to initiate binding, no significant spectral change was seen relative to the unmixed control (data not shown). The data from UV and CD spectra cannot distinguish minor tertiary structure alterations in UCH, and we cannot comment on this possibility solely on their basis. The data do suggest that the electronic environments of the aromatic side chains are not radically altered by ubiquitin binding. Above 340 nm, the lack of UV absorption is consistent with the absence of chromophoric prosthetic groups in the enzyme. The spectra of UCH-L3 yield a Beer−Lambert extinction coefficient of 21 000 L/mol cm at 280 nm. UCH-L1 exhibits similar spectral characteristics, with an extinction of 15 600 L/mol cm. These data are consistent with the expected extinction based on the aromatic content of the polypeptides.

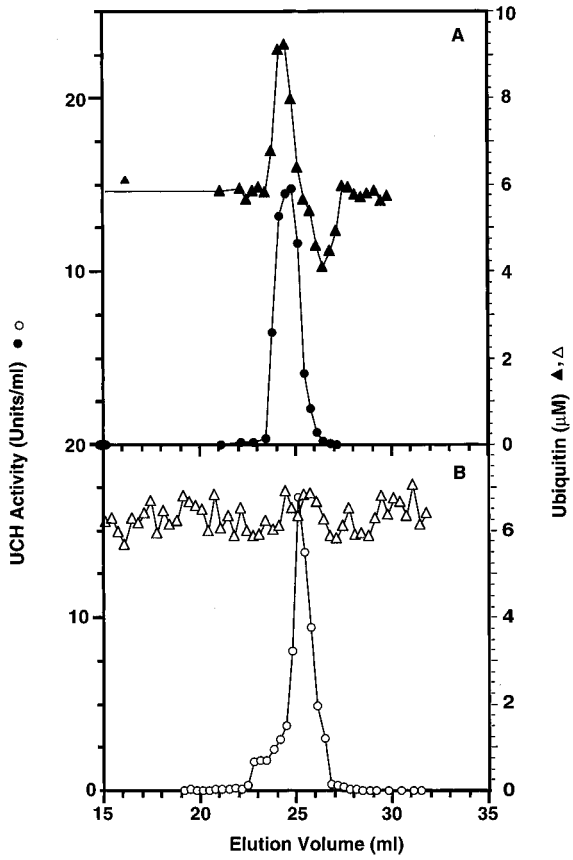

FIGURE 2: Binding of ubiquitin to UCH-L3. Tandem Superose gel permeation columns were equilibrated with 5.8 μM ubiquitin, and a sample of UCH-L3 containing the same concentration of ubiquitin was applied. The effluent was assayed for ubiquitin (triangles) and UCH-L3 enzyme activity (circles). Panel A, results obtained in standard buffer. Panel B, the same except in the presence of 0.5 M NaCl.

Binding of ubiquitin to UCH-L3 was not detectable by any of the spectral methods used above. Nonetheless, kinetic evidence predicts a sub-micromolar binding constant (Wilkinson *et al.*, 1986). Additionally, it is known that the enzyme is specifically bound to and eluted from a ubiquitin affinity column (Duerksen-Hughes *et al.*, 1989; Pickart & Rose, 1985). The kinetically obtained K_m must not be interpreted as a substrate dissociation constant, and the ubiquitin affinity column cannot be used to quantify the binding strength. Thus a direct gel filtration approach was used to monitor this binding. In these experiments, the column buffer is equilibrated with ligand ubiquitin and the enzyme sample is supplemented with an equal concentration of ligand. If binding occurs, one expects to observe a peak of ligand at the elution position of the enzyme and a depressed level of ligand at the included volume of the column. Figure 2A shows that purified UCH-L3 is 91% occupied by ubiquitin when chromatographed in the presence of 5 μM ubiquitin-containing buffer. Integration of the peak area shows that 3.45 nmol of ubiquitin was bound to the 3.80 nmol of UCH-L3 applied. An apparent binding constant of 0.5 μM can be calculated from these data. This is similar to the K_m for UbOEt (Wilkinson *et al.*, 1986) and implies that most of the binding energy is due to ubiquitin alone and not the ester functionality. These data demonstrate that UCH-L3 possesses only one binding site with a micromolar K_d and that the stoichiometry of binding is 1:1.

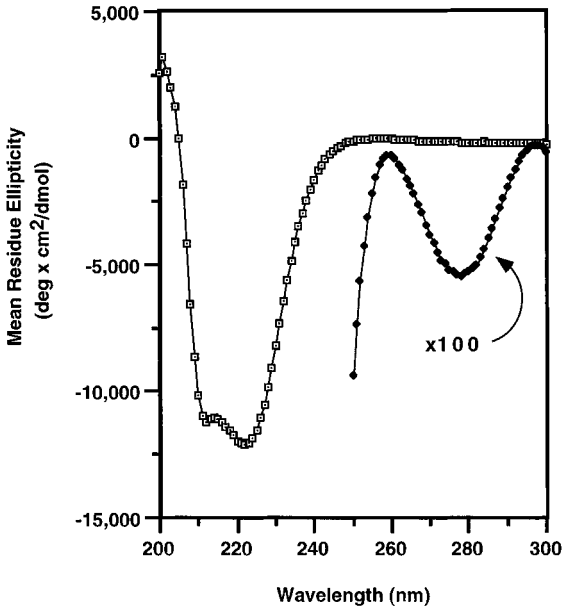

FIGURE 3: Circular dichroism spectra of UCH-L3. Open symbols, 0.95 mg of protein/mL, 1 mm path length; Closed symbols, 0.95 mg of protein/mL, 10 mm path length. The latter spectrum has been multiplied by 100 to show details.

The above data demonstrate the binding of ubiquitin to UCH-L3 and suggest that there are few gross structural changes associated with this binding. Further, the environment of aromatic residues is not greatly perturbed. This suggests that polar interactions may be important for the binding. Indeed, we have noted that increased ionic strength inhibits hydrolysis of ubiquitin ethyl ester (data not shown). This inhibition is virtually complete at 10 μM substrate and 0.40 M NaCl. To examine if the inhibition by ionic strength was due to decreased substrate binding, or to a change in the catalytic properties of the protein, we have repeated these binding experiments in the presence of inhibitory levels of salt. Ubiquitin binding is completely abrogated in the presence of 0.5 M NaCl (Figure 2B). The structure of the enzyme is not grossly perturbed by the presence of salt, as the CD spectra of UCH-L3 in 0 and 0.5 M NaCl are virtually identical (not shown). These data suggest that the binding interactions of the enzyme and substrate are primarily electrostatic and not hydrophobic.

Spectroscopic Analysis of UCH-L3. Circular dichroism spectroscopy was used to estimate the amount of secondary structure motifs in UCH isozymes and mutants (Figure 3) and to evaluate the effects of mutation on the folded protein structure. The CD spectra show an absolute minima at 222 nm, characteristic of the presence of α-helices. This is also confirmed by the relative minima at 208 nm and absolute maxima at 202 nm (Johnson, 1988). Calculating the mean residue ellipticity at 208 and 222 nm, we obtain values of 12 090 and 9160 deg cm^2/dmol, respectively. Using the sum of structures constraint (Greenfield & Fasman, 1969) these values predict α-helix contents of 31.2% and 32.4%. Also shown in Figure 3 is the near-UV dichroism due to the chiral environment of the aromatic residues (curve labeled ×100). As is typical, this region shows much less ellipticity (~60 deg cm^2/dmol), but since this region might serve as an environmentally sensitive reporter for the aromatic residues we have shown it.

Finally, classical nonresonance laser Raman spectroscopy was also used as a structural probe. Figure 4 shows the

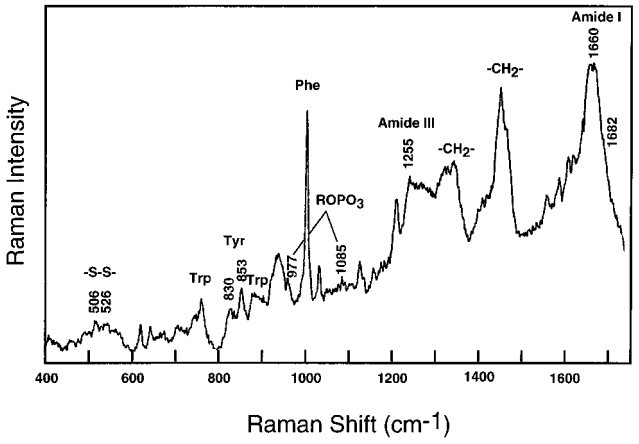

FIGURE 4: Raman spectra of UCH-L3. The spectrum from 400 to 1750 cm^{-1} is shown, and several regions of interest are noted. Details are given in the text.

Raman spectra of UCH-L3 from 400 to 1750 cm^{-1}. We used two methods to calculate the amounts of structural motifs which are based on the conformationally sensitive nature of the peptide carbonyl stretch absorbance. The spectral bandwidth, intensity, and position of this amide I Stokes emission were used to estimate quantities of four generic secondary structures: helix, β-sheet, turn, and random (Alix *et al*., 1981). This method suggests 48% helical content, 25% β-sheet, 16% turn, and 11% "other". Another method (Lippert *et al*., 1976) uses the spectral characteristics (1240, 1632, and 1660 cm^{-1} transitions) of pure helix, β-sheet, and random forms of poly L-lysine to calculate the secondary structure content. Our data predict 40% helix, 43% β-sheet, and 17% random coil when analyzed in this way, but this method cannot distinguish between β-turn and β-sheet motifs. These predictions therefore concur generally with predictions based on Alix *et al*. (1988) and also with the CD data presented above. Weighting the Raman, CD, and prediction algorithms equally, approximate averages of 38% helix, 22% β-sheet, 18% turn or loop, and 19% "nonordered" secondary structures are obtained. Minor discrepancies between the methods may arise as a consequence of the "sum of structure" constraints or from the nature of the model compounds used as the basis for the various computations described above.

Our data show that UCH isozymes possess both helix and β-sheet motifs, similar to the papain family of thiol proteases. To date, the solution crystal structures of five thiol proteases have been solved. Three of these, papain, calotropin D1, and actinidin, are from plant sources; two others, liver cathepsin B and the interleukin 1-β-converting enzyme "ICE", are from mammalian sources [reviewed by Walker *et al*. (1994)]. These enzymes differ from the all-β-chymotrypsin class of serine proteases in both catalytic residues and overall structure. ICE and subtilisin both possess helical content, however, and exhibit an antiparallel β-sheet core domain. While UCH enzymes resemble the papain family members in size and secondary structure content, sequence comparison with the papain family suggests that the UCH family should be classified as a distinct gene family. The solution of a UCH crystal structure would provide a valuable addition to the small collection of α/β-proteases, and these experiments are ongoing.

Thermal Denaturation. The above results demonstrate that the recombinant enzymes and mutants display normal

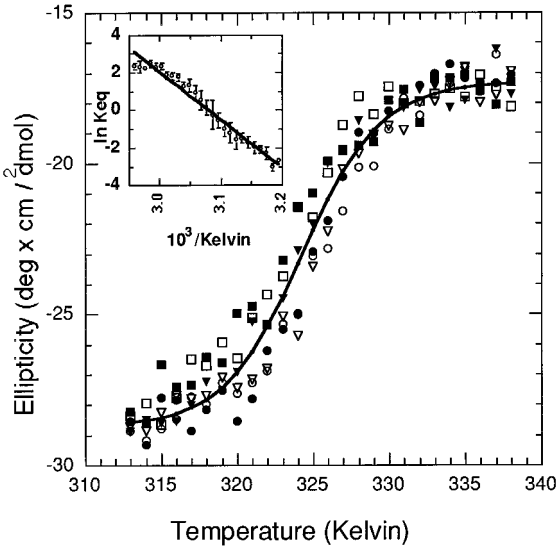

FIGURE 5: Temperature dependent denaturation of wild type UCH-L1 monitored by circular dichroism. Denaturation of wild type UCH-L1. Starting at 40 °C, three independent samples of protein (0.1 mg/mL) were warmed by 1 °C increments and equilibrated for 60 s, and the ellipticity was recorded before the temperature was increased (solid symbols). After reaching 65 °C, the protein was cooled by 1 °C increments and equilibrated for 60 s, and the ellipticity was recorded before the temperature was decreased (open symbols). The solid line drawn through the points is the best fit to the data assuming a single reversible transition. The inset shows the Arrhenius plot of the data. The circles are calculated from the mean of the six observations at each temperature, and the error bars delineate the standard error of the mean.

spectroscopic properties at room temperature. This suggests that all mutants tested fold correctly and are soluble under these conditions. However, the temperature of the enzymatic assay and normal physiological environment of these enzymes is 37 °C. To demonstrate that the loss of activity was due to a direct effect and not irreversible unfolding of the enzymes at assay temperature, we have conducted thermal denaturation experiments monitoring the 222 nm circular dichroism signal. Using this technique, the thermodynamics of protein denaturation have been studied for several enzymes [Alexander *et al*., 1992; reviewed by Privalov and Gill (1988)]. This method provides a powerful, general tool for assessing the structural stability of enzymes and mutants. Figure 5 shows the temperature-dependent changes in the 222 nm CD signal of UCH-L1. As can be seen, there is a thermal transition at approximately 52 °C resulting in a 45% diminishment in this conformationally sensitive signal. UCH-L3 is also subject to the same transition, though the loss of ellipticity is slightly less. Cooling the sample results in the restoration of the original spectra, and wavelength scans at 65 °C are typical of proteins with high random coil content (not shown). Also, the transition is fully reversible if the protein concentration is less than 100 μg/mL (10 μg/mL for H161K and H161Y) and if the protein is not allowed to remain denatured for more than 5 min before the temperature is lowered.

These data can be analyzed according to a two-state model, and the relevant thermodynamic parameters can be calculated. The inset to Figure 5 shows the Arrhenius plot of the data. As obtained from the replot, this transition is characterized by values of $\Delta H = 1.56$ kJ/mol of residue, $\Delta S = 4.80$ J/K mol of residue, and $\Delta G = 28.6$ kJ/mol of UCH-L1 at 25 °C. It is assumed that this transition is the reversible

Table 2: Thermodynamics of Denaturation of UCH's[a]

enzyme	melting point (T_m, ±0.2 °C)	enthalpy, ΔH (kJ/mol of aa)	entropy, ΔS (J/K mol of aa)	Gibbs energy, ΔG (kJ/mol of UCH)
UCH-L3	50.9	1.15	3.52	21.7
UCH-L1	51.8	1.56	4.80	28.6
UCH-L1 C90S	51.5	1.55	4.78	27.7
UCH-L1 H161D	49.9	1.50	4.69	22.6
UCH-L1 H161K	52.7	1.07	3.30	19.1
UCH-L1 H161Y	52.7	1.10	3.40	19.2

[a] Melting points are derived from the primary denaturation data. Thermodynamic values for denaturation are calculated as described in the text, where ΔH = kJ/mol of amino acid residue, ΔS = J/K mol of amino acid residue, and ΔG = kJ/mol of UCH at 25 °C. Conventions are according to Privalov (1979).

denaturation of UCH. The rather modest stability of this protein is consistent with the reversible folding of a single domain protein. Many small globular proteins exhibit folded states stabilized by only 20−60 kJ/mol of Gibbs free energy (Privalov, 1979).

We also performed this thermodynamic analysis for the UCH-L3 isozyme and the L1 isozyme mutants C90S, H161D, H161K, and H161Y. In general the wild-type and mutant enzymes have virtually indistinguishable circular dichroism spectra (not shown) and only slightly differing denaturation curves. All denature at 50−53 °C, where the melting point is defined as that point in the thermal denaturation curve where $K_{eq} = 1$, i.e., the midpoint. Thermodynamic values thus derived are shown in Table 2. By comparison, the neuron specific UCH-L1 appears slightly more stable than its hemopoeitic homologue, UCH-L3. Wild type L1 and the isoelectronic mutant C90S both show virtually identical melting points and thermodynamic stabilities per residue (Privalov & Gill, 1988) with $\Delta G = 28.6$ and 27.7 kJ/mol at 25 °C, respectively. Mutations at the catalytic histidine were only slightly destabilizing, as determined by a melting point depression (H161D) or unfavorably altered thermodynamic state functions (H161K and H161Y). On the basis of these data, we conclude that the inactivity of the C90 and H161 mutants is due to the loss of important catalytic residues and not due to misfolding or a decreased stability of the folded form.

CONCLUSIONS

This is the first detailed analysis of the interaction of ubiquitin with one of its physiological binding sites. We have presented data to demonstrate that cysteine 90 and histidine 161 are the active site nucleophile and general base involved in UCH-L1 catalysis. These data assist in crystallographic model building, as the two residues must be juxtaposed in the tertiary structure and will define the active site. It can also be safely assumed that the other isozymes of the UCH family possess the same catalytic chemistry and residues, for reasons described above. The electronic nature of the binding suggests that one of two faces of ubiquitin is involved in an extensive interaction with this enzyme. One face has been defined as an "acidic face" with many such clustered on the surface of the α-helix from residues 20 to 34. Many of the basic residues are clustered on the opposite face of the molecule. It is not immediately obvious which face is contacting the surface of the enzyme, although there are several approaches which could be pursued to further define this. It is interesting to note that the majority of amino acid substitutions across species occur in the "acidic" face of ubiquitin (Wostmann *et al*., 1992), and for this reason, we assume that the "basic" face is involved in these binding interactions. Data from Burch and Haas (1994) suggest that R42 of ubiquitin is involved in recognition by UCH-L3. Also, the aspartate in the conserved ELDGR box may be involved in the binding. The effect of the D176N mutation on the Michaelis constant for ubiquitin shows that this residue may participate in an ionic interaction with ubiquitin or provide minor "orienting" effects for the fine tuning of substrate positioning. Rose and Warms (1983) have also shown that the two C-terminal glycine residues are necessary for effective inhibition of UCH-L3 by ubiquitin. We find that the attachment of a hexahistidine motif to the N-terminus of ubiquitin does not affect hydrolysis rates to any measurable extent (not shown).

In summary, our data suggest that UCH isozymes (a) utilize cysteine 90 as the nucleophile, (b) use histidine 161 as the general base catalyst, (c) bind ubiquitin electrostatically, (d) bind the intact ubiquitin C-terminus, (e) may possess a carboxylate P3 binding pocket for arginine, (f) do not bind the amino terminus of ubiquitin, (g) bind other basic residues in ubiquitin, and (h) utilize several of UCH's acidic residues in binding. These hypotheses will be useful in building models of the enzyme for crystallographic and structural studies, for defining the enzyme−substrate interaction, and in site-directed mutagenesis experiments designed to alter recognition and specificity of these enzymes.

ACKNOWLEDGMENT

We thank Kwok To Yue (Emory University, Department of Physics) for assistance with obtaining Raman spectra of UCH-L3.

REFERENCES

Alexander, P., Fahnestock, S., Lee, T., Orban, J., & Bryan, P. (1992) *Biochemistry 31*, 3597.
Alix, J. P., Pedanou, G., & Berjot, M. (1988) *J. Mol. Struct. 174*, 159.
Baker, R. T., Tobias, J. W., & Varshavsky, A. (1992) *J. Biol. Chem. 267*, 23364.
Beltramini, M., Bubacco, L., Salvato, B., Casella, L., Gullotti, M., & Garofani, S. (1992) *Biochim. Biophys. Acta 1120*.
Blazy, B., Baudras, A., & Maurizot, J. C. (1992) *Biochim. Biophys. Acta 1120*, 223.
Burch, T., & Haas, A. (1994) *Biochemistry 33*, 300.
Day, I. N. M., Hinks, L. J., & Thompson, R. J. (1990) *Biochem. J. 268*, 521.
Deveraux, Q., Ustrell, V., Pickart, C., & Rechsteiner, M. (1994) *J. Biol. Chem. 269*, 7059.
Duerksen-Hughes, P., Williamson, M., & Wilkinson, K. D. (1989) *Biochemistry 28*, 8530.
Eytan, E., Ganoth, D., Armon, T., & Hershko, A. (1989) *Proc. Natl. Acad. Sci. U.S.A. 86*, 7751.
Finley, D., Ozkaynak, E., & Varshavsky, A. (1987) *Cell 48*, 1035.
Finley, D., Bartel, B., & Varshavsky, A. (1989) *Nature 338*, 394.
Fox, T., Mason, P., Storer, A., & Mort, J. S. (1995) *Protein Eng. 8*, 53.
Greenfield, N., & Fasman, G. (1969) *Biochemistry 8*, 4108.
Grobler, J. A., Wang, M., Pike, A. C. W., & Brew, K. (1994) *J. Biol. Chem. 269*, 5106.
Higgins, D. G., & Sharp, P. M. (1989) *Comput. Appl. Biosci. 5*, 151.
Hough, R., Pratt, G., & Rechsteiner, M. (1987) *J. Biol. Chem. 262*, 8303.

Hummel, J. P., & Dreyer, W. J. (1962) *Biochim. Biophys. Acta 63*, 530.
Johnson, W. C. (1988) *Ann. Rev. Biophys. Chem. 7*, 145.
Kajimoto, Y., Hashimoto, T., Shirai, Y., Nishino, N., Kuno, T., & Tanaka, C. (1992) *J. Biochem. 112*, 28.
Kunkel, T. A. (1985) *Proc. Natl. Acad. Sci. U.S.A. 82*, 488.
Lippert, J. L., Tyminski, D., & Desmeules, P. J. (1976) *J. Am. Chem. Soc. 98*, 7075.
Liu, C. C., Miller, H. I., Kohr, W. J., & Silber, J. I. (1989) *J. Biol. Chem. 264*, 20331.
Lowe, J., McDermott, H., Landon, M., Mayer, R. J., & Wilkinson, K. D. (1990) *J. Pathol. 161*, 153.
Matsui, S., Sandberg, A. A., Negoro, S., Seon, B. K., & Goldstein, G. (1982) *Proc. Natl. Acad. Sci. U.S.A. 79*, 1535.
Mayer, A., & Wilkinson, K. D. (1989) *Biochemistry 28*, 166.
Orsi, B. A., & Tipton, K. F. (1979) *Methods Enzymol. 63*, 159.
Ozkaynak, E., Finley, D., Solomon, M. J., & Varshavsky, A. (1987) *EMBO J. 6*, 1429.
Papa, F. R., & Hochstrasser, M. (1993) *Nature 366*, 313.
Pickart, C. M., & Rose, I. A. (1985) *J. Biol. Chem. 260*, 7903.
Pickart, C. M., & Rose, I. A. (1986) *J. Biol. Chem. 261*, 10210.
Privalov, P. L. (1979) *Adv. Protein Chem. 33*, 205.
Privalov, P. L., & Khechinashvili, N. N. (1974) *J. Mol. Biol. 86*, 665.
Privalov, P. L., & Gill, S. J. (1988) *Adv. Protein Chem. 39*, 191.
Privalov, P. L., & Makhatadze, G. I. (1990) *J. Mol. Biol. 213*, 385.
Rost, B., & Sander, C. (1993) *Proc. Natl. Acad. Sci. U.S.A. 90*, 7558.
Sanger, F., Nicklen, S., & Coulson, A. (1977) *Proc. Natl. Acad. Sci. U.S.A. 74*, 5463.
Sambrook, J., Fritsch, E. F., & Maniatis, T. (1989) in *Molecular Cloning: A Laboratory Manual*, Section 1.72−73, Cold Spring Harbor Press, Cold Spring Harbor, NY.
Schechter, I., & Berger, A. (1967) *Biochem. Biophys. Res. Commun. 27*, 157.
Tobias, J. W., & Varshavsky, A. (1991) *J. Biol. Chem. 266*, 12021.
Vaaler, G. L., & Snell, E. E. (1989) *Biochemistry 28*, 7306.
Vuillemier, S., Sancho, J., Loewenthal, R., & Fersht, A. (1993) *Biochemistry 32*, 1030.
Walker, N. P. C., Talanian, R. V., Brady, K. D., Dang, L. C., Bump, N. J., Ferenz, C. R., Franklin, S., Ghayur, T., Hackett, M. C., Hammill, L. D., Herzog, L., Hugunin, M., Houy, W., Mankovich, J. A., McGuinness, L., Orlewicz, E., Paskind, M., Pratt, C. A., Reis, P., Summani, A., Terranova, M., Welch, J. P., Xiong, L., Moller, A., Tracey, D. E., Kamen, R., & Wong, W. W. (1994) *Cell 78*, 343.
Wilkinson, K. D. (1995) *Annu. Rev. Nutr. 15*, 161.
Wilkinson, K. D., Cox, M. J., Mayer, A. N., & Frey,T . (1986) *Biochemistry 25*, 6644.
Wilkinson, K. D., Lee, K., Deshpande, S., Duerksen-Hughes, P., Boss, J., & Pohl, J. (1989) *Science 246*, 670.
Wilkinson, K. D., Larsen, C. N., & Deshpande, S. (1992) *Biochem. Soc. Trans. 20*, 631.
Wilkinson, K. D., Tashayev, V. L., O'Connor, L. B., Larsen, C. N., Kasperek, E., & Pickart, C. M. (1995) *Biochemistry 34*, 14535.
Wostmann, C., Tannich, E., & Bakker-Grunwald, T. (1992) *FEBS Lett. 308*, 54.
Zhang, N., Wilkinson, K. D., & Bownes, M. (1993) *Dev. Biol. 157*, 214.

BI960099F